LORIST, M. M., BOKSEM, M. A. & RIDDERINKHOF, K. R. (2005). Impaired cognitive control and reduced cingulate activity during mental fatigue. Brain Res Cogn Brain Res 24, 199-205.

CARTER, C. S., BRAVER, T. S., BARCH, D. M., BOTVINICK, M. M., NOLL, D. & COHEN, J. D. (1998). Anterior cingulate cortex, error detection, and the online monitoring of performance. Science 280, 747-749.

JOYNER, M. J. & COYLE, E. F. (2008). Endurance exercise performance: the physiology of champions. J Physiol 586, 35-44.

GENDOLLA, G. H. E. & WRIGHT, R. A. (2005). Motivation in social settings: studies of effort-related cardiovascular arousal. In Social motivation: conscious and unconscious processes. ed. FORGAS, J. P., WILLIAMS, K. D. & LAHAM, S. M., pp. 71-90. Cambridge University Press, Cambridge.

WALTON, M. E., BANNERMAN, D. M., ALTERESCU, K. & RUSHWORTH, M. F. (2003). Functional specialization within medial frontal cortex of the anterior cingulate for evaluating effort-related decisions. J Neurosci 23, 6475-6479.

Authors have confirmed where relevant, that experiments on animals and man were conducted in accordance with national and/or local ethical requirements.

C95

Organisation of microtubules in mpkCCD$_{c14}$ cells

M.I. Smye and D. Marples

Institute of Membrane and Systems Biology, University of Leeds, Leeds, UK

Microtubules (MT) are dynamic, polar structures which mediate a number of essential cellular functions, including vesicle transport. In Madin-Darby Canine Kidney cells, MT networks reorganise as the cells become polarized (Bacallao et al, 1989), with their minus ends in the apical pole. Consistent with this, vesicles carrying aquaporin 2 (AQP2) to the apical surface of collecting duct cells have dynein, a minus-end directed motor, attached. We investigated MT organisation in mpkCCDc14 cells, a cell line derived from murine cortical collecting duct principal cells (Bens et al 1999).

Cells were seeded onto both coverslips and polycarbonate filters, and grown in modified DMEM medium. In some experiments cells were treated with 1nM desmopressin (dDAVP) for 4-5 days to induce AQP2 expression. After three hours washout, half the cells were treated with dDAVP for 30 minutes to induce shuttling. Cells were fixed with either ice cold methanol (-20 °C) or 4% paraformaldehyde, fluorescently labelled using antibodies against α tubulin, γ tubulin, acetylated tubulin, AQP2 and end binding protein 1 (EB1) in various combinations, and viewed using deconvolution and confocal microscopy. All findings described below were confirmed on at least 2 independent preparations.

As expected, cells grown on coverslips were not polarised, did not express AQP2, and displayed a fibroblastic appearance. Labelling for α tubulin revealed a basket weave pattern with the MT organised around the nucleus. Polarisation was seen in the filter-grown cells, although a proportion of fibroblastic cells were also present. Polarised cells were considerably taller than the fibroblastic cells. Labelling for α tubulin revealed a meshwork of MT in the apical part of the cell; microtubules could also be seen running down the lateral borders of the cell alongside the nucleus. Gamma tubulin, found in the centrioles and microtubule organising centre (MTOC), was located apically, usually as two foci. Co-labelling for γ and acetylated α tubulin (characteristic of cilia) confirmed the presence of primary cilia, with an associated basal body. After acute dDAVP treatment, labelling with EB1, which associates with microtubule plus ends, was most abundant in an apical meshwork, but was also seen at the bottom of the cell. Cells not acutely treated with dDAVP had a similar pattern, but a less prominent apical network, suggesting fewer new MTs forming in this region. In fibroblastic cells plus ends were located throughout, with no clear focus. AQP2 labelling was predominantly apical in cells acutely treated with dDAVP.

Our results are consistent with the hypothesis that microtubule assembly is initiated primarily in the apical part of the cells, with plus ends projecting towards the basolateral membrane. Hence dynein will move AQP2-containing vesicles towards the apical surface.

Bacallao, R. *et al.* (1989). *J Cell Biol*, **109**, 2817-2832.

Bens, M. *et al.* (1999) *J Am Soc Nephrol*, **10**, 923-934.

We thank Drs. M. Peckham, E. Morrison, and C. Johnson for advice and antibodies.

Authors have confirmed where relevant, that experiments on animals and man were conducted in accordance with national and/or local ethical requirements.

C96

The regulation of Na^+ transport in H441 cells by AMPK and PI(4,5)P_2

O.J. Mace[1], A.M. Woollhead[2] and D.L. Baines[1]

[1]Basic Medical Sciences, St. George's, University of London, London, UK and [2]Pharmacy and Biomolecular Sciences, University of Brighton, Brighton, UK

The amiloride-sensitive epithelial Na^+ channel, ENaC, composed of α, β and γ subunits controls the fluid lining the airways. Overexpression of ENaC is linked to the pathogenesis associated with cystic fibrosis (Mall *et al*., 2004). We have shown that the AMP mimetic, AICAR, activates the metabolic sensor AMP-activated protein kinase (AMPK) and inhibits amiloride-sensitive Na^+ transport in H441 human lung epithelial cells (Woollhead *et al*., 2005). Its mechanism of action is unknown. As PI(4,5)P_2 is reported to be required for ENaC activation (Kunzelmann *et al*., 2005), we have investigated the hypothesis that AMPK converges on PI(4,5)P_2 and alters ENaC-PI(4,5)P_2 interactions.

Monolayers were mounted in Ussing chambers in physiological salt solution. AICAR (2 mM) rapidly reduced amiloride-sensitive short circuit currents ($I_{SC\text{-}Amil}$) by 49.0 ± 7.6 % ($P < 0.05$, $n = 8$). Compound C, an inhibitor of AMPK, rescued $I_{SC\text{-}Amil}$. Purinergic stimulation by UTP (100 μM) inhibited $I_{SC\text{-}Amil}$ by 49.2 ± 7.5 % ($P < 0.05$, $n = 8$) via depletion of membrane PI(4,5)P_2. Neomycin (5 mM), which sequesters PI(4,5)P_2, inhibited $I_{SC\text{-}Amil}$ by 59.7 ± 12.6 % ($P < 0.05$, $n = 8$) and there was no further inhibition with UTP. Western blotting showed that there

was no change in apical abundance of the α, β or γ ENaC subunits. U-73122 (10 μM), an inhibitor of phospholipase C, elevated $I_{SC\text{-}Amil}$ 1.3 fold ($P = 0.13$, $n = 4$) and AICAR inhibited the elevated $I_{SC\text{-}Amil}$ by 47.7 ± 5.6 % ($P < 0.05$, $n = 4$). Treatment with either UTP or neomycin followed by AICAR further reduced $I_{SC\text{-}Amil}$ to 72.9 ± 4.0 % and 77.1 ± 7.1 % (both $P < 0.05$, $n = 4$), respectively. In these situations, the abundance of αENaC was diminished by 75 ± 7.6 % and that of βENaC by 61 ± 7.6 % (both $P < 0.01$, $n = 4$). There was no change to the apical abundance of the γ ENaC subunit. $PI(4,5)P_2$ co-immunoprecipitated α, β and γ ENaC subunits. However, following treatment of monolayers with AICAR, $PI(4,5)P_2$ only co-immunoprecipitated αENaC and αENaC was barely detectable following treatment with UTP.

The data indicate that activation of AMPK by AICAR or compromising the ENaC-$PI(4,5)P_2$ interaction inhibit the open probability of ENaC. Together, AICAR and the absence of the ENaC-$PI(4,5)P_2$ interaction inhibit amiloride-sensitive Na^+ transport which is paralleled by α and β ENaC subunit retrieval. $PI(4,5)P_2$ interacts with all three ENaC subunits and we hypothesise that this interaction is important for subunit surface expression. We propose that channel subunit retrieval by AMPK is dependent on the $PI(4,5)P_2$ concentration being low, as would be the case in physiological situations in which PLC signaling pathways are operative. It would appear that using $PI(4,5)P_2$ to regulate activity as well as trafficking means that ENaC would only be active at the membrane and not during insertion into or retrieval from the cell surface.

Mall M *et al*. (2004) *Nat Med*. **10**, 487-493.

Woollhead AM *et al*. (2005) *J Physiol*. **1**, 781-792.

Kunzelmann K *et al* (2005) *FASEB J*. **19**, 142-143.

This work was supported by the BBSRC.

Authors have confirmed where relevant, that experiments on animals and man were conducted in accordance with national and/or local ethical requirements.

C97

Expression of SLC15 family proton-coupled peptide transporters in the human A549 lung cell line

M. Paul-Smith[1], M. Pieri[1,2], H. Christian[1] and D. Meredith[2]

[1]Physiology, Anatomy & Genetics, University of Oxford, Oxford, UK and [2]Department of Life Sciences, Oxford Brookes University, Oxford, UK

It is known that the surfactant-secreting alveolar type II (ATII) pneumocytes can mediate peptide transport and express the proton-coupled peptide transporter PepT2 (SLC15A2, reviewed in Meredith & Boyd 2000). The human A549 cell line is believed to be derived from ATII cells, based on shared morphological and biological features including the expression of surfactant genes. The aim of this study was to investigate peptide transporter expression and function in A549 cells.

A549 cells were cultured in F12 medium with 5% CO_2 at 37°C. RNA preparation and RT-PCR were performed using primer sequences for PepT1 and PepT2 and methods as previously reported (Liu *et al.* 1995; Meredith *et al.* 2002). Caco-2 cells were used as a positive control for the PepT1 PCR reaction. A549 cells were fixed in 4% paraformaldehyde/PBS and embedded in LRGold resin for electron microscopy and immunogold detection of PepT1 and PepT2 with polyclonal antibodies for PepT1 (Panitsas *et al.* 2006) and PepT2 (Autogen Bioclear UK). In addition, transport experiments were performed on A549 cells grown to a confluent monolayer on 6-well plates. The culture medium was replaced with 0.4μM [^{3}H]-D-Phe-L-Gln in pH5.5 Krebs, in the absence or presence of 25mM Gly-L-Gln.

RT-PCR studies showed that A549 cells expressed PepT2, but not PepT1 (Figure 1A) and the identity of the PepT2 band was confirmed by sequencing. In positive control Caco-2 cells PepT1 expression was confirmed while a negative control RT-PCR (no RNA template) gave no bands (data not shown). Despite the presence of PepT2 RNA, A549 cells did not show any evidence of mediated transport for the model dipeptide [^{3}H]-D-Phe-L-Gln (Figure 1B). Under the same conditions, Caco-2 cells showed PepT1 mediated transport (data not shown). However, this apparent anomaly was explained when the distribution of PepT2 was examined by immunogold electron microscopy, as most of the immunogold labelling was found to be intracellular. In agreement with the RT-PCR results, no specific immunogold labelling for PepT1 was observed (data not shown).

In conclusion, like the ATII cells, A549 cells express PepT2 but not PepT1. Most of the PepT2 protein in A549 cells was detected intracellularly and no dipeptide uptake was measured, in contrast to ATII cells in which PepT2 activity at the plasma membrane has been demonstrated (Groneberg *et al.* 2001). Although the lack of PepT1 expression in A549 cells argues against the idea of being able to target lung cancer cells with a PepT1-specific anticancer prodrug, we will investigate other lung cancer cell lines in future studies.

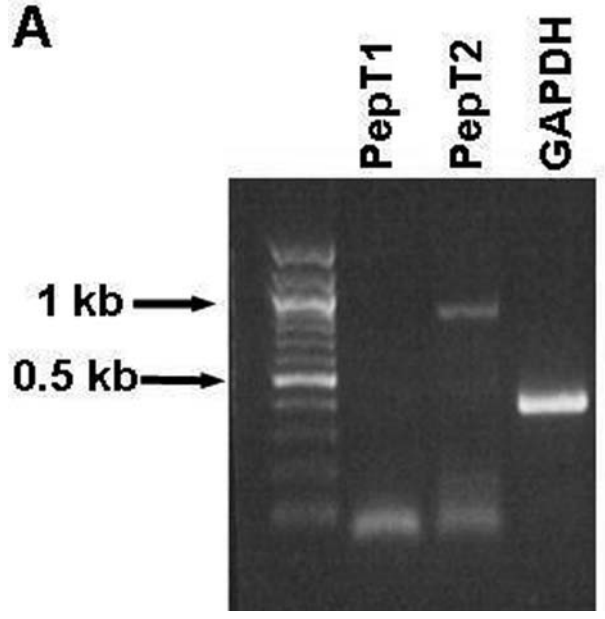

Figure 1A: RT-PCR for PepT1, PepT2 and GAPDH in A549 cells (1% TAE agarose gel).

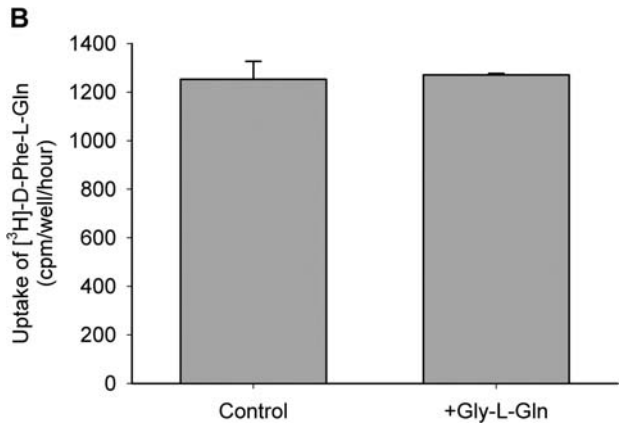

Figure 1B: Uptake of [^{3}H]-D-Phe-L-Gln into A549 cells in the absence or presence of 25mM Gly-L-Gln (n=3 wells per condition, 1 hr uptake).

Meredith D & Boyd CAR (2000) *Cell Mol Life Sci* **57**, 754-578

Meredith D *et al.* (2002) *Cell Physiol & Biochem* **12**, 227-234

Liu W *et al.* (1995) *Biochem Biophys Acta* **1235**, 461-466

Panitsas KE *et al.* (2006) *Pflugers Arch* **452**, 53-63

Groneberg DA *et al.* (2001) *Am J Pathol* **158**, 707-714

We are grateful to Cancer Research UK for their support

Authors have confirmed where relevant, that experiments on animals and man were conducted in accordance with national and/or local ethical requirements.

C98

Influenza A virus NS1 protein-induced Na^+ conductance in human bronchiolar (H441) cells

M. Gallacher[1], S.G. Brown[1], B.G. Hale[2], R.E. Olver[1], R.E. Randall[2] and S.M. Wilson[1]

[1]Lung Membrane Transport Group, University of Dundee, Dundee, UK and [2]Centre for Biomolecular Sciences, University of St Andrews, St Andrews, UK

Influenza is a major worldwide respiratory pathogen responsible for seasonal epidemics and occasional worldwide pandemics. Influenza infection can lead to an accumulation of fluid in the respiratory tract, implying that the virus can modulate the ion transport in these tissues. Previous work has shown influenza infection acutely modulates Na^+ absorption by inhibiting the epithelial sodium channel (ENaC) (Kunzelmann *et al.* 2000). Recent work has shown that influenza A NS1 protein can activate host cell intracellular phosphatidylinositol-3-kinase (PI3K) (Hale *et al.* 2006). Since this enzyme is involved in the regulation of ENaC expression, we have examined the effect of NS1 expression on Na^+ conductance (G_{Na}) in the H441 human bronchiolar cell model. G_{Na} in H441 cells grown in hormone free conditions is negligible, but can be stimulated by treatment with the glucocorticoid hormone dexamathasone (Clunes *et al.* 2004). Here we report a G_{Na} recorded from voltage clamped H441 human epithelial cells stimulated by the transfection of influenza A NS1 protein. In control, hormone free, cells (GFP only) the resting membrane potential (V_m, -61.7 ± 2.4 mV) was unaltered by lowering external sodium. Expression of NS1 depolarized V_m to -22 ± 2.2 mV. Lowering $[Na^+]_o$ to 10 mM hyperpolarized this V_m to -43.1 ± 2.6 mV indicating that G_{Na} is significant. Analysis of the external sodium-dependant component of the membrane current indicated an NS1 induced G_{Na} of 455 ± 165 pS/cell. Expression of NS1-Y89F, a mutant unable to activate 3-phosphatidylinositol phosphate kinase (PI3K) (Hale *et al.* 2006), also induced G_{Na} of magnitude 258 ± 53 pS cell 1 which was smaller ($P < 0.05$) than in cells expressing wild type NS1. Expression of NS1-Y89F in combination with membrane-anchored PI3K P110a subunit induced G_{Na} of magnitude 458 ± 158 pS/cell thus recovering the response of WT-NS1. NS1 expression can therefore mimic the effect of glucocorticoid stimulation by inducing G_{Na} and ~50% of this response can be attributed to an effect upon PI3K.

Clunes M *et al.* (2004). *J Physiol* **557**, 809-819.

Hale BG *et al.* (2006). *PNAS* **103**, 14194-14199.

Kunzelmann K *et al.* (2000). *PNAS* **97**, 10282-10287.

Authors have confirmed where relevant, that experiments on animals and man were conducted in accordance with national and/or local ethical requirements.

C99

Key role of CFTR for all modes of intestinal HCO_3^- secretion

A.K. Singh[1], W. Zheng[1], M. Sjöblom[1,2] and U. Seidler[1]

[1]Gastroenterology, Endocrinology and Hepatology, Hannover Medical School, Hannover, Germany and [2]Neuroscience, Uppsala University, Uppsala, Sweden

Background: CF patients suffer from a variety of gastrointestinal problems, which may all be directly or indirectly linked to the inability of intestinal mucosa to secrete HCO_3^- and to inhibit Na^+/H^+ mediated fluid absorption and proton secretion. This has led to an intense search for alternative modes of intestinal anion transport, and expressions of a variety of potential alternative intestinal anion transporters have been reported.
Aim: To delineate the dependency of different modes of intestinal HCO_3^- secretion on CFTR expression.
Methods and Results: We studied acid-, agonist- and HCO_3^- stimulated as well as Cl^--dependent HCO_3^- secretion in the $CFTR^{tm1cam}$ and WT murine duodenum *in vivo*. NHE3 and Slc26a6-deficient mice were used for selected questions. Luminal acid, forskolin, heat-stable *E. coli* enterotoxin (STa), PG E2, carbachol, and an increase of blood HCO_3^- all stimulated duodenal HCO_3^- secretion in anesthetized (10 µl/g I.P. haloperidol/midazolam/fentanyl cocktail (haloperidol 12.5 mg/kg, fentanyl 0.325 mg/kg and midazolam 5 mg/kg body weight)) WT but not in $CFTR^{tm1cam}$ mice. Pharmacological inhibition or genetic ablation of NHE3 resulted in a significantly higher basal HCO_3^- secretory rate, which was electroneutral and therefore due to an unmasking of apical Cl^-/HCO_3^- exchange activity. Accordingly, Slc26a6 ablation attenuated S1611-induced $J_{HCO}3^-$. Removal of luminal Cl^- reverted basal HCO_3^- secretion to H^+ secretion, but surprisingly, forskolin was able to elicit a full HCO_3^- secretory response. In the absence of CFTR, electroneutral NaCl

absorptive rates were similar to WT rates, but S1611 induced virtually no increase in HCO_3^- secretion.
Conclusion: This indicates that the apical anion exchangers Slc26a6 and Slc26a3 need proton recycling via NHE3 to operate in the Cl^- absorptive mode, and Cl^- exit via CFTR to operate in the HCO_3^- secretory mode. In addition, Cl^- independent HCO_3^- secretion can be stimulated by cAMP increase, likely from the crypt reagion, which expresses high levels of CFTR but none of the anion exchangers.

Hogan DL *et al*. (1997). *Gastroenterology* **113**, 533-541.

Hogan DL *et al*. (1997). *Am J Physiol Gastrointest Liver Physiol* **272**, G872-G878.

Seidler U *et al*. (1997). *J Physiol* **505**, 411-423.

Furukawa O *et al*. (2004). *Am J Physiol Gastrointest Liver Physiol* **286**, G102-9.

Tuo BG *et al*. (2006). *Gastroenterology* **130**, 349-358.

Authors have confirmed where relevant, that experiments on animals and man were conducted in accordance with national and/or local ethical requirements.

C100

Towards *in vivo* correction of the *cftr* ΔF508 allele: design and synthesis of two zinc finger nucleases for homology-directed repair

C.M. Lee[1], R. Flynn[1,2] and P.T. Harrison[1]

[1]Physiology, University College Cork, Cork, Ireland and [2]Department of Medicine, University of Washington, Seattle, WA 98195-7710, WA, USA

Cystic fibrosis (CF) affects 1 in 4000 individuals. Most CF patients have the ΔF508 mutation in the *cftr* gene which disrupts an apical membrane chloride channel. Virus vector-mediated gene replacement therapy has not succeeded. Attempts to repair, rather than replace the defective gene, have been thwarted by the extremely low efficiency of homologous recombination (1 in 100.000 cells). In 2005, Urnov and colleagues designed a pair of zinc finger nucleases (ZFNs) to induce a double stranded break at a unique genomic site, and showed that co-transfection of the ZFNs with a donor repair sequence resulted in homology-directed repair (HDR) of a target allele in up to 20% of transfected cells (1). This level of HDR has been independently confirmed (2), and the system can be delivered by virus vectors (3). We describe a pair of ZFNs (ZFN1 and ZFN2) that target the *cftr* gene, as a first step towards *cftr* gene correction. Two ZF proteins were designed and synthesised to independently recognise two 9 bp sequences, separated by a 4 bp spacer. The combined sequences corresponds to a 22 bp region of intron 9 in the *cftr* gene, close to the ΔF508 site. The DNA sequence of each ZF protein was fused inframe with the nuclease domain of FokI (4) in pcDNA 3.1+ (InVitrogen). Recombinant proteins (ZFN1 and ZFN2) were produced in a coupled transcription-translation reaction (Promega). Two 9 bp target sequences (t1 and t2) were assembled together and cloned into pGL3 (Promega) to mimic the *cftr* gene sequence (pTarget1/2), or duplicated separately (pTarget1/1 and pTarget 2/2) to test efficacy and specificity of individual ZFNs. Target DNA (1000ng) was mixed with 10, 50 and 100ng ZFN protein and incubated for 1 hr at 37°C in enzyme buffer #2 (New England Biolabs). ZFN1 and ZFN2 together linearised pTarget1/2 at all amounts tested. ZFN2 alone cleaved pTarget2/2 but not pTarget1/1. In contrast, ZFN1 alone cleaved pTarget1/1, but not pTarget2/2. Thus, initial data suggested the ZFNs were behaving as predicted. However, some non-specific cleavage was observed when high levels of ZFN were used: 100ng ZFN1 could partially cleave pTarget1/2. Recent studies have suggested that non-specific binding and cleavage can be prevented by mutation of the nuclease domains (5). Introduction of these mutations (QuikChange site-directed mutagenesis; Stratagene) into ZFN1 (to create $ZFN1^{++}$) and ZFN2 (to create $ZFN2^{--}$) prevented non-specific cleavage. In summary, a pair of ZFNs can specifically bind and cleave an 18 bp sequence in the *cftr* gene close to the ΔF508 site. They will be used with a suitable donor sequence to determine the efficiency of ZFN-mediated homology directed repair in a $\Delta F508^{-/-}$ cell line.

Urnov FD et al. (2005). Nature 435:646-51.

Szczepek M et al. (2007). Nat Biotechnol. 25:786-93.

Lombardo A et al. (2007). Nat Biotechnol. 25:1298-306.

Wu J et al. (2007). Cell Mol Life Sci. 64:2933-44.

Miller JC et al., (2007). Nat Biotechnol. 25:778-785.

HEA PRTLI and Dept of Physiology for funding, Miriam O'Sullivan for technical support, and Prof. S. Chandrasegaran for ZFN vector.

Authors have confirmed where relevant, that experiments on animals and man were conducted in accordance with national and/or local ethical requirements.

C101

Trafficking of the cystic fibrosis transmembrane conductance regulator (CFTR) to the cell surface

Y. Luo, I.R. Bates and J.W. Hanrahan

Physiology, McGill University, Montreal, QC, Canada

CFTR is a membrane glycoprotein which functions as an anion channel in exocrine epithelia and is mutated in the disease cystic fibrosis (CF). The most common disease causing mutation, deletion of a phenylalanine at position 508 (ΔF508), causes partial misfolding and retention of CFTR in the endoplasmic reticulum. This misprocessing reduces the amount of complex glycosylated CFTR ("band C") detected in Western blots, and glycosylation is often used to assay maturation of the protein after exposure to low temperature (eg 29 °C) or chemical chaperones. However core-glycosylated CFTR may also reach the plasma membrane after rescue and contribute to anion conductance. Recent attempts to demonstrate this trafficking have relied on conventional cell surface biotinylation by sulfo-NHS-SS-biotin. We examined this surface biotinylation method and found that core-glycosylated ΔF508-CFTR was labelled and pulled down on streptavidin beads, as were several intracellular proteins including the R domain of CFTR expressed in the

cytosol as a soluble polypeptide. The R domain was detected in <1 % of cellular protein, similar to the fraction of cells that were permeable to ethidium homodimer-1 in live/dead cell assays, therefore the cytoplasmic aspect of CFTR is probably labelled by sulfo-NHS-SS-biotin in a subpopulation of leaky cells that are undergoing normal cell turnover.

To study the trafficking of small quantities of immature protein to the cell surface more definitively, we inserted a target sequence for enzymatic biotinylation in the fourth extracellular loop of CFTR and ΔF508-CFTR. These constructs were specifically labelled on the cell surface and protected intracellularly within the lumen of the secretory pathway. Low temperature and chemical chaperones restored some channel activity but yielded little band C; most enzymatically-biotinylated ΔF508-CFTR that reached the plasma membrane was the immature "band B" glycoform. We then used live cell imaging to identify possible routes of CFTR trafficking. Secreted proteins usually move from exit sites in the endoplasmic reticulum (ER) to the cis-Golgi via tubulovesicular structures which comprise the ER-Golgi intermediate compartment (ERGIC), however total internal reflection fluorescence (TIRF) microscopy revealed ER-localized CFTR surprisingly close to the plasma membrane (<200 nm). The lectin ERGIC-53, a cargo carrier for glycosylated proteins, was used as an ERGIC marker. Two colour TIRF imaging revealed a close association between CFTR-mCherry and ERGIC-53-EGFP in mobile vesicles that were transported towards the cell periphery. These results suggest a mechanism for trafficking CFTR channels to the plasma membrane which bypasses the Golgi apparatus and may explain delivery of immature, core-glycosylated CFTR to the cell surface.

CCFF & CIHR (Breathe Program) to JWH, CIHR fellowship to IRB.

Authors have confirmed where relevant, that experiments on animals and man were conducted in accordance with national and/or local ethical requirements.

C102

Nucleotides and phosphatase substrates bind at separate sites on pig kidney Na,K-ATPase

O. Fatola, K. Tsioulos and J.D. Cavieres

Cell Physiology and Pharmacology, University of Leicester, Leicester, UK

Besides ATP, the sodium pump can hydrolyse phosphatase substrates like *p*-nitrophenyl phosphate (*p*NPP) in the presence of K ions; ATP, ADP, and their analogues act as low-affinity competitive inhibitors of the K^+-phosphatase activity. Covalent block of an N-domain pocket (1) by FITC abolishes high-affinity ATP binding, ATP phosphorylation and the Na,K-ATPase activity, but the phosphatase activity and the low-affinity nucleotide effects remain (2,3). FITC modification aside, this effect on *p*NPP hydrolysis reflects the prominent low affinity ATP activation and ADP inhibition of the Na,K-ATPase activity. In fact, with our purified Na,K-ATPase preparations we now realise that ADP can be a better inhibitor (K_i of 0.27-0.42 mM) than ATP is an activator ($K_{0.5}$ of 0.6 mM). We wished to find out, therefore, whether the low affinity ATP and ADP effects on the Na,K-ATPase activity resulted from direct binding at the phosphatase substrate site.

We applied two kinetic tests. If the substrate concentration is held fixed, increasing inhibitor concentrations should yield linear Dixon plots (1/v vs. [i]) if substrate and inhibitor compete for a unique site. However, we find that at 0.6 mM *p*NPP, the Dixon plot is clearly hyperbolic with ATP concentration, with a $K_{0.5}$ of 8.6 mM. This is diagnostic of partially competitive inhibition (4): at the saturating concentration, ATP will have unhindered access to the nucleotide site whilst *p*NPP may still bind at a distinct phosphatase site from time to time. The high fitted $K_{0.5}$ value should signal the ATP binding affinity at the nucleotide site when *p*NPP occupies the phosphatase site (4). The second test involves the use of 2 inhibitors, to decide whether they bind at the same or different sites to cause the inhibition. We plotted the reciprocal of the K^+-phosphatase activity at a fixed 6 mM *p*NPP, as a straight line against 4-methylumbellipherone phosphate concentration (0-3 mM); this is another phosphatase substrate and a full competitor. The same was done again, but now in the presence of 4 mM ADP. Both straight lines were clearly convergent on the left, which indicates that the ternary complex is possible, of the pump with 4-methylumbellipherone phosphate and ADP. Mutual exclusion of the two inhibitors would have shown as roughly parallel straight lines (5). Finally, we did the converse experiment, and measured Na,K-ATPase activity at a fixed 0.25 mM ATP. The reciprocal of the ATPase activity was plotted against 0-2 mM ADP, with and without 15 mM *p*NPP. The straight lines were again clearly convergent on the left. Taken together, these results strongly suggest that the K^+-phosphatase substrates bind elsewhere and not at the locus where nucleotides modulate the pump activities. Long-range effects should be the main cause for the mutual decrease in binding affinities.

Morth, J.P. *et al.* (2007) Nature **450**, 1043-1050.

Ward, D.G. & Cavieres, J.D. (1998) J. Biol. Chem. **273**, 14277-14284.

Ward, D.G. & Cavieres, J.D. (2003) J. Biol. Chem. **278**, 14688-14697.

Cleland, W.W. (1970) In *The Enzymes* (P.D. Boyer, ed.), Vol II, pp. 1-65. N.Y. (Academic).

Yonetani, T. & Theorell, H. (1964). Arch. Biochem. Biophys. **106**, 243-251.

Supported by grants from The Wellcome Trust.

Authors have confirmed where relevant, that experiments on animals and man were conducted in accordance with national and/or local ethical requirements.

C103

Interaction between purinergic and cholinergic signalling in urinary bladder smooth muscle

M.E. Werner[1], T.J. Heppner[2] and M.T. Nelson[1,2]

[1]Cardiovascular Science, University of Manchester, Manchester, UK and [2]Department of Pharmacology, University of Vermont, Burlington, VT, USA

Introduction: The urinary bladder has two major functions, the storage and voiding of urine. The first requires relaxation of the

PC157

Experimental arthritis-induced skeletal muscle wasting is associated with increased proteolysis but not with decreased myogenesis

E. Castillero, M. Granado, A. Martín, M. López-Menduiña, A. López-Calderón and M. Villanúa

Physiology, Complutense University of Madrid, Madrid, Spain

Experimental arthritis is an animal model of chronic inflammation that induces cachexia and skeletal muscle atrophy. It has been previously reported that during acute and chronic phases of the desease there is an increase of muscular protein degradation by the ubiquitin-proteasome pathway. Potential changes in myogenesis during arthritis-induced cachexia have not been studied. The aim of this work was to analize the effect of adjuvant-induced arthritis on markers of muscle regeneration. For this purpouse, arthritis was induced in male Wistar rats by an intradermal injection of Freund's adjuvant in the sole of the paw. The clinical symptoms of arthritis began 10 days after the injection, and the highest arthritis index was reached on day 22. Arthritic and control rats were humanly killed on days 10, 15 and 22 after the adjuvant injection. In the arthritic rats gastrocnemius relative weight was not modified on day 10, it decreased on day 15 ($P<0.01$), and it was markedly lower on day 22 ($P<0.01$). Arthritis induced a marked increase in serum interleukin-6 concentrations and in gastrocnemius ubiquitin ligase muscle-RING-finger protein 1 (MuRF-1) gene expression on all days studied, specially on day 15 ($P<0.01$). Neither of muscular diffentiation markers myogenin or miogenic differentiator 1 (MyoD) were decreased in arthritic rats. On the contrary, arthritis increased myogenin expression on days 15 and 22 ($P<0.01$), and MyoD expression on all days studied ($P<0.05$). Muscular proliferating cell nuclear antigen (PCNA) expression was also increased on days 15 and 22 in arthritic rats.These data suggest that arthritis-induced muscle wasting is mediated by increased proteolysis, but not by decreased myogenesis.

This work was supported by CYCYT (Ref: BEFI2003-02149), a grat to E. Castillero (Gobierno Vasco, BFI06.31) and a grant to M. Lopez-Menduiña (BFU, 2006-11899)

Authors have confirmed where relevant, that experiments on animals and man were conducted in accordance with national and/or local ethical requirements.

PC158

Involvement of ENaC in the initiation of signaling events leading to decidualization/implantation in Mice

Y. Ruan[1,2], W. Zhou[2] and H. Chan[1]

[1]Epithelial Cell Biology Research Center, Li Ka Shing Institute of Health Sciences, Department of Physiology, the Chinese University of Hong Kong, Hong Kong, China and [2]School of Life Science, Sun Yat-sen University, Guangzhou, China

The endometrium undergoes an indispensable differentiation process – decidualization in embryo-implantation. While the maternal-embryo cross-talk in initiating decidualization remains largely unknown, it has been cleared that the endometrial epithelium is required. Our previous studies have demonstrated that the endometrial epithelial expression of ENaC is enhanced during implantation and that intrauterine injection of ENaC blocker, amiloride, inhibits the implantation rate in mice, indicating the potential role of the epithelial ENaC in implantation. Interestingly, serine proteases, the reported ENaC activity-modulating factors, are known to be required for implantation and also, have been shown to promote the release of PGE2 from many epithelial cells, which has been demonstrated to play crucial roles in decidualization. Thus, we hypothesized that ENaC may be involved in the initiation of PGE2 release from endometrial epithelial cells leading to decidualization. In the present study, endometrial epithelial cells of mice were primarily cultured and grown on semipermeable membranes for forming polarized monolayers. Trypsin, a serine protease, aprotinnin, the protease inhibitor and amiloride, the ENaC blocker, were added to the culture medium, and the release of PGE2 to basolateral compartment was detected using an EIA kit. The results showed that, incubating with trypsin (20μg/mL) for 10 min could significantly enhance the PGE2 level in the treated cells as compared to the untreated control. While pretreated the cells with amiloride (10μM) or aprotinin (20μg/ml) for 30 min reversed the effect of trypsin. These results have demonstrated the involvement of ENaC in the release of PGE2 from endometrial epithelial cells, indicating its potential role in decidualization. Thus, ENaC appears to be essential to implantation.

The work was supported by the National 973 projects (2006CB504002 and 2006CB944002), the Strategic Investment and Li Ka Shing Institute of Health Sciences of The Chinese University of Hong Kong, and the Morningside Foundation

Authors have confirmed where relevant, that experiments on animals and man were conducted in accordance with national and/or local ethical requirements.

PC159

Functional characterisation of novel aquaporins from the European Eel *Anguilla Anguilla*

K. Walton[1], C.P. Cutler[3], N. Hazon[2], G. Cramb[2] and G. Cooper[1]

[1]Biomedical Science, University of Sheffield, Sheffield, UK, [2]School of Biology, University of St Andrews, St Andrews, UK and [3]Department of Biology, Georgia Southern University, Statesboro, GA, USA

The European Eel is a euryhaline teleost, which is able to adapt to survive in a fresh or seawater environment. The aquaporin water channels play important roles in osmoregulation in both mammals and fish. Recently it was shown that seawater adaptation leads to changes in the expression levels of the aquaporins eAQP1 and eAQP3 (Lignot *et al*.,2002, Martinez *et al*., 2005). Screening of eel cDNA libraries highlighted two putative clones with high homology to mammalian AQP8, which we have labelled eAQP8 and eAQP8b. In the current study we have investigated the permeability properties of the eel aquaporins, eAQP1, 3, 8 and 8b. The cDNA encoding the eel proteins eAQP1, eAQP3, eAQP8 and eAQP8b was subcloned into the Xenopus expression vector

pTLN (Lorenz *et al*., 1996) and cRNA prepared. Oocytes were isolated from humanely killed Xenopus laevis, and injected with 5ng (0.1ng/nl) cRNA encoding the appropriate aquaporin or 50nl of H_2O. Experiments were performed at room temperature on day 3 or 4 following injection. Uptake of urea was performed as described previously (Fenton *et al*., 2000). Osmotic water permeability (Pf) was calculated from the rate of volume change upon exposing the oocytes to a hypotonic solution. Methylammonium (MA) uptake was performed in a fashion similar to that for urea uptake, with the oocytes exposed to a solution containing 20μM MA chloride supplemented with 1μCi/ml 14C MA chloride for 15 minutes. Statistical analysis was performed using unpaired t-tests or one way ANOVA coupled with Dunnett's test. Statistical significance has been assumed at the 5% level.

The results are summarised in Table 1. We saw a significant increase in Pf in oocytes expressing eAQP1, 8 and 8b, indicating that these proteins act as water channels. eAQP3 and 8 caused significant increases in urea permeability. In addition oocytes expressing eAQP1 and eAQP3 exhibited a significant increase in MA permeability compared to control, suggesting that eAQP1 and eAQP3 also provide a pathway for NH_3 across the cell membrane.

The aquaporins fall into two classes the 'classical' aquaporins and aquaglyceroporins. Our results suggest that eAQP1 and eAQP8b have permeability properties similar to the classical aquaporins, while eAQP3 and eAQP8 fit into the aquaglyceroporin class.

Table 1.

	Pf ($x10^{-3}$ cm.s^{-1})	Urea Uptake (pMol.oocyte.$90s^{-1}$)	MA uptake (pMol.oocyte.$900s^{-1}$)
Control	12.0 ± 5.8(7)	6.2±1.0 (15)	1.5±0.2 (7)
eAQP1	89.7±10.2 (7)**	12.4±1.3(15)	2.5±0.2 (7)*
eAQP3	25.7±1.8 (4)	70.7±3.8(12)*	2.3±0.2 (8)*
eAQP8	69.5±17.4 (6)**	70.6±6.6(15)*	1.8±0.2 (8)
eAQP8b	44.0±5.4 (6)**	12.8±2.0(12)	1.8±0.1 (6)

Values are presented as mean ± SEM with the number of observations in parentheses. * denotes $p<0.05$ compared to the control group as judged by one way ANOVA, and * * indicates $p<0.05$ versus the control group as judged by an unpaired t-test.

Lignot *et al*. (2002). J.Exp.Biol. **205**, 2653-2663.

Martinez *et al*. (2005). Am.J.Physiol. **288**, R1733-R1743.

Lorenz *et al*. (1996). P.N.A.S. **93**, 13362-13366.

Fenton *et al*. (2000). Am.J.Physiol. **279**, C1425-C1431.

The financial support of NERC is gratefully acknowledged.

Authors have confirmed where relevant, that experiments on animals and man were conducted in accordance with national and/or local ethical requirements.

PC160

The expression of CFTR and SLC26A6 in cultured prostate epithelial cells of rats and their involvement of pH regulation

C. Xie and H. Chan

The Chinese University of Hong Kong, Hong kong, China

CFTR and SLC26A6 have been previously demonstrated to be expressed in the male and female reproductive systems and play an important role in pH regulation. However their expression and function in the prostate are unclear. To investigate this, the present study established a primary culture of rat ventral prostate epithelium grown on permeable supports and the expression of CFTR and SLC26A6 was determined by RT-PCR, western blot and immunostaining. The results obtained by these methods consistently showed the expression of CFTR and SLC26A6 in rat prostate epithelial cells. Experiments were also carried out to demonstrate the involvement of CFTR and SLC26A6 in pH regulation across the cultured prostate epithelial cells by fluorimetric intracellular pH measurements using the pH-sensitive fluorescent dye BCECF-AM. The results showed that the pH recovery from alkalization could be altered by forskolin (10μM) and NPPB (100μM), agents known to active and inhibit CFTR, respectively. The physiological function of both CFTR and SLC26A6 in the rat prostate epithelium and their possible involvement in the pathogenesis of prostate diseases await further studies.

Quinton, P. M. (2001). Nature Med. 7, 292–293.

Wang XF et al. (2003).Nat Cell Biol.5(10):902-6.

Shigeo Taketa. (1990) .Prostate. 17(3):207-18.

Hihnala S. (2006). Mol Hum Reprod. 12(2):107-11.

Kujala M. (2007).Reproduction. 133(4):775-84.

Authors have confirmed where relevant, that experiments on animals and man were conducted in accordance with national and/or local ethical requirements.

PC161

Insulin augments glucocorticoid-induced α-ENaC expression via the mammalian target of rapamycin (mTOR)

G.B. Watt and S.C. Land

Maternal and Child Health Sciences, Dundee University, Dundee, UK

Fluid clearance from the lung is critical for breathing to begin at birth and defects in this process can cause lasting impairment of lung function. This process is stimulated by a rise in circulating glucocorticoids before birth which drive expression and recruitment of epithelial Na^+ channel (ENaC) subunits to the epithelial membrane. Previous work has shown that the glucocorticoid effect is, however, malleable, and can be augmented by other hormones such as insulin (1). Thus, kinases in the insulin signalling cascade must be involved in promoting glucocorticoid-dependent ENaC expression. The aim of this study was to determine if the mammalian target of rapamycin (mTOR), a kinase involved in insulin signalling, participated in the insulin-evoked amplification of glucocorticoid regulated Na^+ transport. We focussed on the expression of αENaC as the major pore forming subunit of the ENaC channel. H441 cells maintained under serum free conditions were transfected with a luciferase reporter gene promoted by 2.3kb of the proximal αENaC promoter. A mutant form of the reporter in which the glucocorticoid response element had been mutated was used as a negative control. Cells were treated with either varying concentrations of dexamethasone (Dex; 0-200nM) or a single concentration of Dex (100nM) plus varying concentrations of

insulin (0-1000nM) for 6 hours before harvesting. Luciferase assays revealed the activity of the αENaC promoter and western blotting was performed to determine total cellular αENaC abundance and mTOR activity (phosphorylation of p70S6K-T389). For statistical tests, data were analysed by one-way ANOVA with the level of significance determined by Tukey's test. We found that Dex significantly increases the expression of αENaC, with the average fold change over control 4.94 ± 1.08 SEM (p value = 0.01 at 100nM Dex), and that insulin significantly augments this response (p value = 0.03 at 100nM insulin) with the average fold change over the Dex response 2.8 ± 0.65 SEM. Densometric analysis revealed a significant increase in the phosphorylation of p70S6K (p value = 0.03 at 100nM insulin). Total cellular abundance of αENaC was also increased by insulin (fold change over Dex response = 7.8 at 1nM of insulin). Rapamycin antagonised the insulin effect but failed to alter the expression of αENaC induced by Dex alone. Insulin significantly augments the Dex effect on H441 cells resulting in the increased activity of mTOR. This is paralleled by an increase in the total abundance of αENaC. We suggest that mTOR, a nutrient sensitive kinase, might play a role in the hormonal regulation of ENaC. This may have implications in fluid clearance at birth and also in any tissue expressing ENaC and in the treatments of any diseases resulting from defects of Na^+ homeostasis.

Brown SG, Gallacher M, Olver RE, Wilson SM (2008). The regulation of selective and non-selective Na^+ conductances in H441 human airway epithelial cells. Am J Physiol Lung Cell Mol Physiol Epub ahead of print.

Supported by the George and Sheila Livanos Trust and the Wellcome Trust.

Authors have confirmed where relevant, that experiments on animals and man were conducted in accordance with national and/or local ethical requirements.

PC162

Towards a simple haemolytic test for diagnosing sickle cell disease

J.S. Gibson[1], J. Sarfo-Annin[2] and J.C. Ellory[2]

[1]Veterinary Medicine, University of Cambridge, Cambridge, UK and [2]Physiology, Anatomy and Genetics, University of Oxford, Oxford, Ox, UK

Sickle cell disease (SCD) is one of the commonest inherited diseases, affecting millions of people, particularly in Western Africa but also in the Caribbean, USA and Northern Europe. A simple mutation in the β haemoglobin gene produces HbS, rather than the normal HbA. Most patients are the homozygous HbSS-type, but heterozygotes also display symptoms eg HbSC and HbS-thalassaemia. Deoxy-HbS is less souble and able to form rigid polymers which distort the red cell into bizarre shapes, also producing other sequelae which include increased membrane permeability. The resulting pathology is complex and extensive, involving anaemia and vaso-occlusive episodes, hence pain and organ damage. Early diagnosis is critical to manage and ameliorate the common manifestations of SCD (Steinberg, 2001). The increased membrane permeability of sickle cells involves several pathways (Lew & Bookchin, 2005): KCl cotransport, a deoxygenation-induced non-selective cation pathway(P_{sickle}) and the Gardos or Ca^{2+}-activated K^+ channel. K^+ loss via these pathways induces cells to shrink. The rise in [HbS] makes sickling more likely, with other changes including phospholipid scrambling. P_{sickle} plays a central role by allowing Ca^{2+} entry, activating the Gardos channel. Although the principle defect is mainly increased cation permeability, sickle cells lyse in isosmotic non-electrolyte solutions when deoxygenated in N_2 (Browning *et al* 2007). Lysis is accompanied by entry of non-electrolye into the cells. Here we have developed a simple haemolytic test for diagnosing SCD, which utilises this phenomenon.

Sickle red cells were washed in MOPS-buffered saline (145mM NaCl, 5mM glucose, 10mM MOPS, pH 7.4) and re-suspended in isosmotic sucrose solution (replacing NaCl with sucrose). They were deoxygenated with sodium metabisulphite (4%) rather than by reduction in O_2 tension. After 30 min incubation, unlysed red cells were removed by centrifugation. Haemolysis was determined using Hb measurement as optical density at 540nm or by eye. Under these conditions, in samples from 33 SCD patients (both HbSS and HbSC), haemolysis was present in 29 (88%), compared with 1 in 13 (8%) for normal red cells. The ability to deoxygenate chemically, using haemolysis as a simple measure of increased permeability of sickle cells represents an important step towards developing a novel and practical diagnostic test for SCD, amenable for use in less developed areas of the world. In addition, it also appears that metabisulphite which oxidises the bulk of the haemoglobin to methaemoglobin with its oxy-configuration also supports a permeability change hitherto observed under conditions of low O_2 tension when Hb will be in the deoxy-form.

Browning, J. A., Robinson, H. C., Ellory, J. C. & Gibson, J. S. (2007). Cell. Biochem. Physiol. 19, 165-174.

Lew, V. L. & Bookchin, R. M. (2005). Physiol. Rev. 85, 179-200.

Steinberg, M. H. (1999). New Eng. J. Med. 340, 1021-1030.

We thank the Wellcome Trust and Action Medical Research for financial support.

Authors have confirmed where relevant, that experiments on animals and man were conducted in accordance with national and/or local ethical requirements.

PC163

Rapid effects of hypoxia on pH homeostasis in articular chondrocytes

J.S. Gibson[1], T.P. Fairfax[2], R.J. Wilkins[2] and P.I. Milner[3]

[1]Veterinary Medicine, University of Cambridge, Cambridge, UK, [2]Physiology, Anatomy and Genetics, University of Oxford, Oxford, Ox, UK and [3]Faculty of Veterinary Science, University of Liverpool, Liverpool, UK

As articular cartilage is avascular, their chondrocytes experience low O_2 levels. Values can fall further in chronic disease states. Hypoxia perturbs cell function, inhibiting metabolism and matrix synthesis. It also perturbs ion homeostasis (Gibson *et al.* 2008). Chondrocyte intracellular pH (pH_i) is a powerful

regulator of matrix synthesis. Acid extrusion, largely mediated by Na^+-H^+ exchange (NHE) (Wilkins et al. 2000), is inhibited when cells are incubated for several hours at low O_2, leading to intracellular acidification (Milner et al 2006). O_2-dependent changes in levels of reactive oxygen species (ROS) appear to underlie this effect. The rapidity with which hypoxia exerts these effects is important both mechanistically and for the consequence of short term hypoxia on joint integrity, but it has not been characterised.

Cartilage slices were taken from bovine and equine fetlock joints of animals humanely killed for other purposes. Chondrocytes, isolated by collagenase digestion, were incubated at 20% or 1% O_2 at 37°C. pH_i was determined fluorimetrically with BCECF (Wilkins & Hall, 1992), using NH_4Cl to alter pH_i. ROS levels were determined using DCFH. Salines were buffered with HEPES (10 mM), in nominal absence of CO_2 / HCO_3^- and equilibrated at the required O_2 tension by incubation in tonometers.

Steady state pH_i was maintained for periods of up to 40 min (ΔpH_i = 0.10±0.04, n=3). A step change to 1% O_2 caused a decline in pH_i within 10min, and the fall continued throughout the recording period (Figure 1a). At 1% O_2 in the presence of $CoCl_2$ (100μM), fall in pH_i was largely abolished; at 1% O_2 with the mitochondrial complex III inhibitor antimycin A (100μM), a rapid alkalinisation of pH_i was observed. ROS levels decreased in response to hypoxia (to 60±15% control values, means+SEM, n=3), but were maintained by treatment with either Co^{2+} or antimycin A. Recovery from ammonium-imposed intracellular acidification was also slowed within 10min under hypoxia, via reduction in the Na^+-dependent / HOE694-sensitive component of the acid flux, consistent with a reduction in NHE activity (Figure 1b).

These findings show that hypoxia has rapid effects on chondrocyte function, acidifying cells via NHE inhibition, correlating with alteration in ROS levels. Aside from their obvious implications for chondrocyte homeostasis and cartilage integrity, the rapidity of the response observed here may be of relevance in the context of other hypoxic tissues such as the ischemic myocardium.

Figure 1a

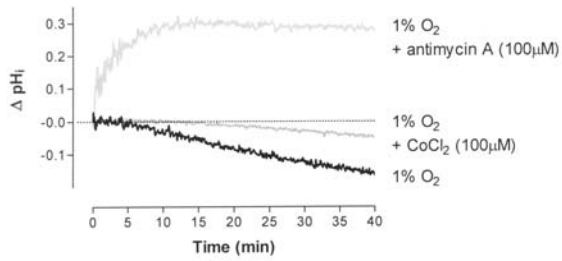

Figure 1b

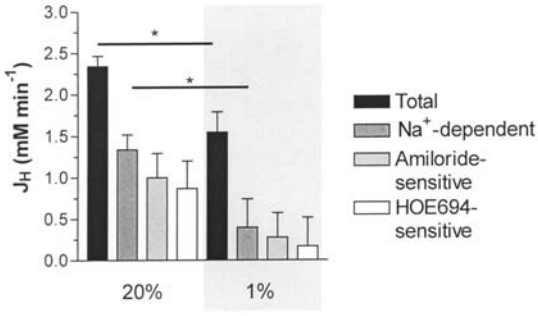

Gibson, J. S., Milner, P. I., White, R., Fairfax, T. P. A. & Wilkins, R. J. (2008). Pflugers Archiv 455, 563-573.

Milner, P. I., Fairfax, T. P. A., Browning, J. A., Wilkins, R. J. & Gibson, J. S. (2006). Arthritis Rheum. 54, 3523-3532.

Wilkins, R. J. & Hall, A. C. (1992). Exp. Physiol. 77, 521-524.

Wilkins, R. J., Browning, J. A. & Ellory, J. C. (2000). J. Membrane Biol. 177, 95-108.

We thank the Horserace Betting Levy Board and the Sir Hailley Stewart Trust for financial support.

Authors have confirmed where relevant, that experiments on animals and man were conducted in accordance with national and/or local ethical requirements.

PC164

Duodenal cytochrome b (Dcytb) functions as a cupric reductase *in vitro*

S. Wyman, R. Simpson, A.T. McKie and P. Sharp

Nutritional Sciences, King's College London, London, UK

Copper is an essential metal, involved in a number of key enzymes in human metabolism. Dietary copper import takes place in the duodenum and requires that the metal is present in its reduced cuprous form. To date the mechanisms involved in the reduction of Cu (II) to Cu (I) are unclear. Like copper, iron must also be present in the reduced Fe (II) form before it becomes bioavailable. This is achieved in part by the presence of the duodenal ferric reductase Dcytb [1]. Given the overlap

between copper and iron metabolism [2], the aim of this study was to determine whether Dcytb might also act as a cupric reductase.

Dcytb was isolated from mouse duodenal mRNA, PCR amplified, and ligated into a pEGFP-N1 vector (Clontech, Palo Alto, USA) to permit to addition of a carboxy terminal enhanced green fluorescent protein (EGFP) tag. The Dcytb-EGFP product was subsequently excised and inserted into pTRE2hyg vector (Clontech) which contains a tetracycline responsive element upstream of a minimal CMV promoter to control expression of Dcytb-EGFP. The plasmid was transfected into MDCK Tet-off cells (Clontech) which allows Dcytb-EGFP expression to be switched off in the presence of doxycyclin (10ng/ml culture medium for 4 days). Stably transfected cells were used to study cupric reductase activity using bathocuprionedisulfonate (BCS). The formation of the Cu (I)-BCS complex was monitored by the change in absorbance at 482nm. Standard curves were generated to convert the absorbance value into pmoles of copper reduced. All reactions were performed in the dark at 37C. Statistical analysis was performed using one-way ANOVA and Tukey's post-hoc test and differences were considered significant at $P<0.05$. Data are mean ± SEM.

MDCK cells over-expressing Dcytb-EGFP protein reduced significantly greater amounts of copper (transfected, 0.70 ± 0.02 pmol/μg cell protein/min; untransfected, 0.07 ± 0.01 pmol/μg cell protein/min; $P<0.001$, n = 6 in each group). Reductase activity was significantly diminished in the presence of doxycyclin (0.37 ± 0.01 pmol/μg cell protein/min; $P<0.01$, n = 6).

These data provide the first evidence that, in addition to its well-characterised role as a ferric reductase, Dcytb also function as a cupric reductase *in vitro*. We are exploring further the role of this enzyme in copper metabolism.

McKie AT *et al*. (2001) *Science* **291**, 1755-1759.

Sharp PA (2004) *Proc Nutr Soc* **63**, 563-569.

This work was funded by project grants from the Biotechnology and Biological Sciences Research Council. SW was supported by a KCL Strategic Studentship.

Authors have confirmed where relevant, that experiments on animals and man were conducted in accordance with national and/or local ethical requirements.

PC165

Ca^{2+} handling in normal and cystic fibrosis human airway epithelial cells

K.L. Harris[1], R. Muimo[2] and L. Robson[1]

[1]*Biomedical Science, University of Sheffield, Sheffield, UK and* [2]*Academic Unit of Child Health, University of Sheffield, Sheffield, UK*

Cystic fibrosis is caused by mutations in the cystic fibrosis transmembrane conductance regulator (CFTR), a Cl^- channel that plays an important role in Cl^- secretion. In the airway CFTR function is regulated by an interaction with annexin-2 and S100A10 (1). This complex is also known to be important in regulating the epithelial Ca^{2+} channels TRPV5 and TRPV6 (2). A recent study has demonstrated that the annexin-2 / S100A10 interaction is lost in CF airway cells (3). Given the fact that TRPV channels are also found in airway, this suggests that Ca^{2+} handling could be altered in CF airway cells. Calcium uptake was measured in 16HBE14o- and CFBE41o- cells grown in 12-well multi-well plates. The buffer solution contained (in mM): 140 NaCl, 5 KCl, 2 $CaCl_2$, 1 $MgCl_2$, 10 HEPES, 10μM felodipine and 10μM verapamil (to inhibit voltage-gated Ca^{2+} channels). Cells were exposed to this solution for 40 minutes, with Ca^{45} (5μCi/ml) added during the final minute. 10μM forskolin (FSK) and 100μM (IBMX) were added during the last 30 minutes. Cells were washed, lysed and Ca^{45} uptake analysed using direct DPM scintillation counting. This was repeated in the presence of 5nM cypermethrin or 100μM ruthenium red (RR). All treatments were day matched and values are expressed as means ± SEM. Statistical significance was tested using the unpaired Students t-test or ANOVAs and assumed at the 5% level. Day matched CFBE41o- cells demonstrated greater Ca^{2+} uptake versus 16HBE14o- cells, 245 ± 17.7 pg/10^5 cells (n=24) versus 199 ± 18.8 pg/10^5 cells (n=24), respectively. Ca^{2+} uptake in both cell types was inhibited in the presence of cypermethrin or RR, Table 1.

These data indicate that in both 16HBE14o- and CFBE41o- cells Ca^{2+} uptake is dependent on a cypermethrin and RR sensitive pathway, which may be attributable to TRPV6. Ca^{2+} uptake was greater in CF cells, suggesting that CFTR plays a role in regulating Ca^{2+} handling. Further work is needed to elucidate the pathway regulated by CFTR and the molecular mechanisms underlying this process.

Table 1: Effect of cypermethrin or RR on Ca^{2+} uptake in day matched cells

pg/10^5 cells	Control	Cypermethrin	Control	RR
16HBE14o-	173 ± 16.7 n=16	98.2 ± 10.7 n=12	229 ± 22.5 n=12	116 ± 24.1 n=11
CFBE41o-	514 ± 38.4 n=18	338 ± 47.0 n=18	284 ± 43.8 n=18	155 ± 25.2 n=18

Borthwick, Mcgaw, Conner, Taylor, Gerke, Mehta, Robson, & Muimo. (2007). The formation of the cAMP/protein kinase A- dependent annexin 2- S100A10 complex with cystic fibrosis conductance regulator protein (CFTR) regulates CFTR channel Function. Molecular Biology of the Cell, 18 (9):3388-97.

van de Graaf, Hoenderop, Gkika, Lamers, Prenen, Rescher, Gerke, Staub, Nilius, & Bindels. (2003). Functional expression of the epithelial Ca2+ channels (TRPV5 and TRPV6) requires association of the S100A10-annexin 2 complex. European Molecular Biology Organization Journal, 22(7): 1478-1487.

Borthwick, Riemen, Goddard, Colledge, Mehta, Gerke & Muimo. (2008). Defective formation of PKA/CnA-dependent annexin 2-S100A10/CFTR complex in deltaF508 cystic fibrosis cells. Cell Signalling. In press

This work was supported by a University of Sheffield Harry Worthington Scholarship.

Authors have confirmed where relevant, that experiments on animals and man were conducted in accordance with national and/or local ethical requirements.

PC166

A genetically-encoded ratiometric sensor to measure extracellular pH in microdomains bounded by basolateral membranes of epithelial cells

L. Cid[1], J. Urra[1], M. Sandoval[1,2], I. Cornejo[1], L. Barros[1] and F.V. Sepúlveda[1]

[1]Centro de Estudios Cientificos (CECS), Valdivia, Chile and [2]Universidad Austral de Chile, Valdivia, Chile

Extracellular pH, especially in relatively inaccessible microdomains between cells, affects transport membrane protein activity and might have an intercellular signaling role. We have developed a genetically encoded extracellular pH sensor capable of detecting pH changes in basolateral spaces of epithelial cells. It consists of a chimerical membrane protein displaying concatenated enhanced variants of cyan fluorescence protein (ECFP) and yellow fluorescence protein (EYFP) at the external aspect of the cell surface. The construct, termed pHCECSensor01, was targeted to basolateral membranes of MDCK cells by means of a sequence derived from the aquaporin AQP-4. The fusion of pH-sensitive EYFP with pH-insensitive ECFP allows ratiometric pH measurements. The titration curve of pHCECSensor01 in vivo had a pKa value of 6.5±0.04. Only minor effects of extracellular chloride on pHCECSensor01 were observed around the physiological concentrations of this anion. In MDCK cells the sensor was able to detect changes in pH secondary to proton efflux into the basolateral spaces elicited by an ammonium prepulse or lactate load. This genetically encoded sensor has the potential to serve as a non-invasive tool for monitoring changes in extracellular pH microdomains in epithelial and other tissues in vivo.

Fondecyt grant 1051081

Authors have confirmed where relevant, that experiments on animals and man were conducted in accordance with national and/or local ethical requirements.

PC167

Electrophysiological evidence for heterogeneity of cell types involved in K^+ and Cl^- secretion in human colonic crypts

J. Linley[1,2], S. Kopanati[1], G.I. Sandle[2] and M. Hunter[1]

[1]Institute of Membrane and Systems Biology, University of Leeds, Leeds, UK and [2]Institute for Molecular Medicine, St. James's University Hospital, Leeds, UK

Although the main function of the colon is salt and water absorption, it has the capacity to secrete substantial amounts of K^+ and Cl in infective and neurohumoral diarrhoeal diseases. Secretion involves movement of ions across the luminal (apical) membrane of colonic crypt cells, K^+ exiting via large conductance K^+ (BK) channels and Cl^- through CFTR. Colonocytes and goblet cells constitute most of the crypt cell mass. It is generally assumed that both K^+ secretion and Cl^- secretion arise from colonocytes in response to the activation of different second messenger cascades, but the relative magnitudes and spatial arrangement of the apical K^+ and Cl^- conductances are unclear.

Intact crypts were isolated from distal colonic biopsies obtained with consent from patients undergoing routine colonoscopy for altered bowel habit, in whom the mucosa was macroscopically and histologically normal. Whole-cell K^+ and Cl^- currents and conductances were measured from the mid-third of colonic crypts using the perforated patch technique (addition of amphotericin B to the pipette). Comparisons were made using Student's t-test. Two distinct cell populations were identified based on the biophysical characteristics, pharmacology and agonist responses of the whole-cell currents. 73% of cells (58/79) had basal inwardly rectifying K^+ conductances (IR), which were $68 \pm 14\%$ ($P<0.05$, $n = 4$) inhibited by clotrimazole (10μM), a blocker of intermediate conductance IK channels, but not by penitrem A (100nM), a blocker of BK channels. In contrast, 27% (21/79) of cells had a basal outwardly rectifying K^+ conductance (OR) which was $68 \pm 6\%$ ($P<0.005$, $n = 8$) inhibited by penitrem A. Stimulating intracellular cAMP activated CFTR in IR cells (whole-cell conductance increasing from 0.97 ± 0.1nS to 3.5 ± 0.5nS, $P<0.0005$, $n = 11$), but had no effect in OR cells (6.6 ± 1.0nS to 7.3 ± 1.0nS, $n = 7$). We conclude that K^+ and Cl^- secretion occur in different cell types within colonic crypts. Given the relative proportions of colonocytes and goblet cells within the human colon, our data suggest that goblet cells are the main site of K^+ secretion, whereas colonocytes are the main site of Cl^- secretion.

The support of Yorkshire Cancer Research is gratefully acknowledged.

Authors have confirmed where relevant, that experiments on animals and man were conducted in accordance with national and/or local ethical requirements.

PC168

Further evidence for the interaction of rabbit PepT1 proteins when expressed in *Xenopus* oocytes

S. Brown[1], M. Pieri[1,2] and D. Meredith[2]

[1]Physiology, Anatomy & Genetics, University of Oxford, Oxford, UK and [2]School of Life Sciences, Oxford Brookes University, Oxford, UK

It has recently been reported that the rabbit proton-coupled peptide transporter PepT1 (SLC15a1) is a functional multimer, with a tetramer (potentially a dimer of dimers) best fitting the experimental data from co-expression of a non-functional expressed mutant W294F-PepT1 and wild-type PepT1 (Panitsas *et al.* 2006). The mechanism by which the mutant PepT1 inhibits the function of the wild-type PepT1 is not known. This study examines whether other non-functional expressed PepT1 mutants can also inhibit wild-type PepT1 when co-expressed in *Xenopus* oocytes. The mutants were in either the same region of PepT1 (E594R, transmembrane domain 10 (TMD10)) or on the opposite side (H57A, TMD2) to W294F (TMD7), based on a recent homology model (Meredith & Price 2006).

The co-expression and analysis of mutant and wild-type PepT1 was as previously reported (Panitsas *et al.* 2006). Mutant PepT1 cRNAs were injected at a molar fraction of 0.75.

The surface expression of the wild-type (FLAG-tagged) PepT1 was not affected by the co-expression of any of the non-functional mutant PepT1 proteins (Figure 1). However, the functional activity of the wild-type PepT1 was affected by the mutant PepT1 proteins (Figure 2). As had been found previously (Panitsas *et al.* 2006), W294F-PepT1 is very effective at inhibiting wild-type PepT1 function. The other mutants tested, E594R- and H57A-PepT1 also produced a significant reduction in the function of the wild-type PepT1, despite not affecting its expression in the oocyte plasma membrane.

This study shows that the interaction of expressed non-functional PepT1 mutants is not unique to W294F-PepT1. The fact that E594R- and H57A-PepT1 were apparently equally as effective in suppressing wild-type PepT1 activity, despite their predicted positions being on opposite sides of the protein from each other (but at the same depth in the TMD) suggests that the effect on the wild-type protein might not be due to where the proteins physically interact with each other. Rather, we hypothesis that the inhibition may be due to the inability of the non-functional protein to undergo the change in shape envisaged during the translocation step in the transporter cycle, when the substrate binding site is re-orientated from facing one side of the membrane to the other.

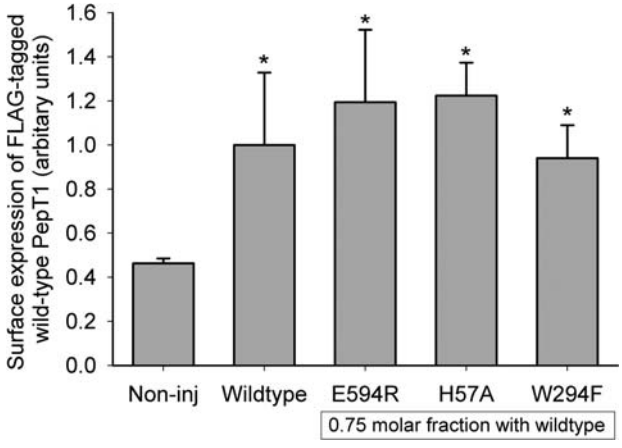

Figure 1: Luminometry results for FLAG-tagged wild-type PepT1 expression in oocytes in the absence and presence of mutant PepT1. Data are mean ± SEM for ≥2 oocyte preparations, with ≥20 oocytes per condition in each. *p<0.05, Student's t-test versus non-injected control oocytes.

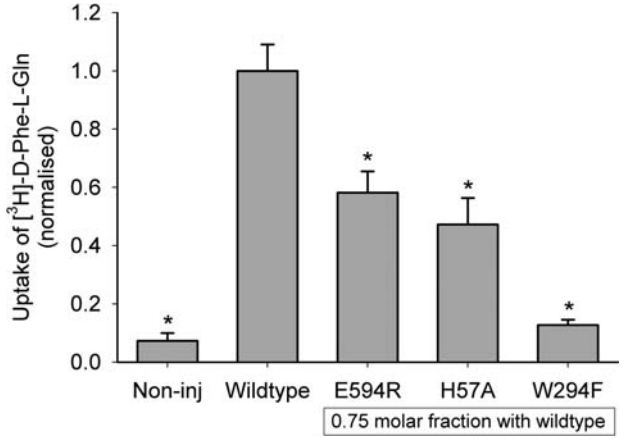

Figure 2: Uptake results for FLAG-tagged wild-type PepT1 expressed in oocytes in the absence and presence of mutant PepT1. Data are mean ± SEM for ≥2 oocyte preparations, with 10 oocytes per condition in each. *p<0.05, Student's t-test versus FLAG-tagged wild-type PepT1.

Panitsas KE *et al.* (2006) *Pflugers Arch* **452**, 53-63

Meredith D & Price RA (2006) *J Memb Biol* **213**, 79-88

We thank the Wellcome Trust for their support.

Authors have confirmed where relevant, that experiments on animals and man were conducted in accordance with national and/or local ethical requirements.

PC169

Effect of dexamethasone on the serum-glucocorticoid-dependent kinase (SGK) and extracellular signal-regulated kinase (ERK) signalling cascades in H441 cells

S.K. Inglis, E. Husband and S. Wilson

Maternal and Child Health Sciences, University of Dundee, Dundee, UK

The epithelial sodium channel (ENaC) is regulated by a number of hormones, including glucocorticoids, mineralcorticoids and insulin. The molecular basis of this control is not clear. We have shown that insulin increases Na^+ conductance (G_{Na}) and amiloride-sensitive short-circuit current in the Na^+-absorbing H441 cell line derived from human distal airways (1). This regulation is dependent on the presence of dexamethasone, which increases the activity of SGK (1). In the absence of dexamethasone there is a basal level of SGK activity that is inhibited by the PI3 kinase blocker, LY294002, but, surprisingly, negligible G_{Na}. We hypothesise that an inhibitory pathway may restrict G_{Na} in the absence of dexamethasone, and that the glucocorticoid may, in addition to activating SGK, inactivate such a pathway. The signalling cascades involving ERK 1 and 2 inhibit ENaC at the transcritional level (2) and by facilitating their removal from the membrane by a Nedd-4-dependent mechanism (3). Thus the aim of this study was to investigate the effect of dexamethasone on ERK activity in H441 cells. Cells were grown on plastic in defined, hormone-free conditions (4). Protein was extracted after drug addition and aliquots were fractionated by SDS-polyacrylamide gel electrophoresis and blotted onto Hybond-P membranes. Western analysis was carried out using antibodies directed against phosphorylated and total ERK. Abundance was assessed using densitometry. Dexamethasone (0.2μM) significantly reduced levels of phospho ERK1 (fig) within 1hour and this inhibition was maintained for 4hr (ANOVA and Dunnets, $p<0.05$, n=9). ERK2 showed the same response pattern. SGK1 activity (assayed by quantifying NDRG1-$Thr^{346/356/366}$ phosphorylation (5), fig) was increased over the same time period (ANOVA and Dunnets, $p<0.05$, n=15). LY294002 (50μM, 2hr) increased phospho-ERK1 (by 89±12%) and ERK2 (by 98±20%) levels (Student's paired t-test, n=3). Total-ERK and total-SGK levels were unaffected in these experiments. Treatment of H441 cells grown on permeable supports into resistive monolayers with the ERK inhibitor, U0126 (0.5μM for 5hr), increased amiloride-sensitive G_{Na} measured in an Ussing chamber (61.1±8.2 to 76.2±6.6μScm^{-2}, $p<0.05$, n=4). These results suggest that ERK signalling inhibits amiloride-sensitive Na^+ conductance in H441 cells and that this pathway is inhibited by dexamethasone. Dexamethasone thus increases G_{Na} by

at least two mechanisms; firstly by activating SGK, and secondly by suppressing the ERK pathway, which is normally inhibitory to G_{Na}.

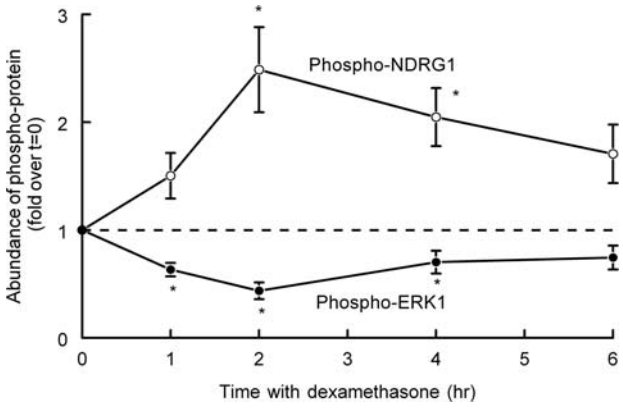

Figure shows abundance of phospho-NDRG1 (n=17)and phospho-ERK1 (n=9) after exposure to dexamethasone for various time periods. Data are normalised to abundance at time zero. Data are mean plus or minus sem.

Inglis SK *et al*. Manuscript in preparation.

Zentner MD *et al*. (1998) J. Biol. Chemistry **273** 30770-30776.

Shi H *et al*. (2002) J. Biol. Chem. **277** 13539-13547.

Brown SG *et al* (2008) Am. J. Physiol. In press.

Murray JT *et al* (2005) Biochem. J. **277** 1-12.

This work was funded by grants awarded by the MRC and Wellcome Trust.

Authors have confirmed where relevant, that experiments on animals and man were conducted in accordance with national and/or local ethical requirements.

PC170

Overexpression of the mTOR-activating protein, Rheb, induces a Na^+ conductance in human lung epithelial cells (H441)

S.G. Brown[1], S.C. Land[2], M. Gallacher[2], R.E. Olver[2] and S.M. Wilson[2]

[1]School of Contemporary Sciences, University of Abertay Dundee, Dundee, UK and [2]Division of Maternal and Child Health Sciences, Ninewells Hospital and Medical School, University of Dundee, Dundee, UK

The active absorption of water from the surface of epithelial cells in the gas exchanging region of the lungs is dependent upon electrogenic Na^+ transport via epithelial sodium channels (ENaC). Regulation of ENaC expression involves the activity of serum and glucocorticoid-dependent kinase-1 (SGK1). Previous evidence suggests that the protein kinase mammalian target of rapamycin (mTOR) may control Na^+ coupled solute transport via an intracellular signalling pathway shared with SGK1 (Shojaieford and Lang, 2006; Shojaieford et al., 2006). The aim of this study was to examine if over expression of a constitutively active mTOR activating protein, Ras homologous enriched in brain (Rheb), induced sodium channel expression in a manner analogous to over expression of SGK1 in single human lung H441 epithelial cells using perforated patch clamp electrophysiology.

Sodium conductance (G_{Na}, $NMDG^+$ substitution) is negligible in cells cultured in hormonally deprived conditions (0.03±0.020 nS $cell^{-1}$). In hormonally deprived, Rheb expressing cells $NMDG^+$ substitution revealed a $[Na^+]_o$ dependent depolarisation of V_m (control: -16.2±2.0mV; low Na^+ -52.4±3.3mV, P<0.001). The Rheb induced Na^+ conductance is rapamycin sensitive (rheb: 1.80±0.7 nS $cell^{-1}$; Rheb + rapamycin 0.51±0.07 nS $cell^{-1}$, P<0.01, n=10). Surprisingly, overexpression of Rheb (D60V), a mutant form that does not bind guanine nucleotides, also induced a sodium conductance (0.21±0.1 nS $cell^{-1}$, n=5). Similar to previous findings (Shojaieford et al., 2006), expression of a catalytically inactive form of SGK1 (K127A) significantly reduced the Rheb induced sodium conductance (Rheb: 1.91±0.41 nS $cell^{-1}$, Rheb + SGK1-K127A 0.41±0.08 nS $cell^{-1}$, P<0.001, n=5). Like the SGK1 induced Na^+ conductance (Brown et al., 2008), the Rheb induced Na^+ conductance in single H441 cells is amiloride insensitive. Thus mTOR and SGK1 may increase G_{Na} through a shared mechanism.

Shojaieford, M and Lang, F. (2006). Biochem. Biophys. Res. Comm. 345, 1611-1614.

Shojaieford, M., Christie, D.L. and Lang, F. (2006). Biochem, Biophys. Res. Comm., 341, 946-949.

Brown, S.G., Gallacher, M., Olver, R.E. & Wilson, S.M. (2008). Am.J.Physiol., Lung Cell Mol. Physiol., epub.

The authors are grateful to the Wellcome Trust and to Tenovus Scotland for their financial support

Authors have confirmed where relevant, that experiments on animals and man were conducted in accordance with national and/or local ethical requirements.

PC171

Properties of HEK-293 cells heterologously expressing TASK-2 cloned from H441 epithelial cells

M.K. Mansley, N. McTavish and S.M. Wilson

Maternal and Child Health Sciences, University of Dundee, Dundee, UK

The airway surface liquid (ASL) adjacent to airway epithelial cells is crucial for normal respiratory function. The composition and volume of the ASL is governed by Na^+ absorption across the epithelial cells. In human bronchiolar epithelial (H441) cells, this Na^+ absorption is dependent on a K^+ conductance that maintains the driving force for Na^+ entry through apical ENaC channels (Inglis *et al.* 2007). This K^+ conductance displays an interesting profile of being insensitive to barium yet sensitive to acid (pH6) and the local anaesthetic bupivacaine. These properties suggest that a two-pore domain K^+ channel (K_2P) may be responsible for this conductance, with the acid-sensitive TASK-2 channel a likely candidate. We therefore cloned TASK-2 from H441 cells and stably expressed it in HEK-293 cells. The purpose of this study is to characterise the pharmacological profile of the conductance associated with the heterologous

expression of TASK-2 in HEK-293 cells using electrophysiological methods.
Whole cell patch clamp recordings revealed an endogenous outward current in untransfected HEK cells (18.1 ± 2.0 pA pF^{-1} at 87mV, n = 33) under quasi-physiological conditions. This current is carried dominantly by K^+ ions as raising $[K^+]_o$ (136mM) increased both inward and outward currents and depolarised the reversal potential (V_{rev}) in the manner predicted by the Goldman-Hodgkin-Katz equation for a selective K^+ conductance. This endogenous current was insensitive to acid (pH6) with an inward current blocked by barium (3mM) and an outward current blocked by bupivacaine (3mM) and TEA (10mM). Heterologous expression of TASK-2 conferred an acid-sensitive outwardly-rectifying current onto HEK cells (43.2 ± 4.4 pA pF^{-1} at 87mV, n = 22). Raising $[K^+]_o$ depolarised V_{rev} similarly to that seen with the endogenous current, confirming the current is carried by K^+ ions. The outward rectification persisted at raised $[K^+]_o$ indicating the channel passes little inward current at very hyperpolarised potentials. The acid sensitivity allowed isolation of the current associated with TASK-2 and initial studies have revealed this acid-sensitive current to be insensitive to 10mM TEA. However, the magnitude of this current was only double that of the endogenous current and the complex nature of these native currents makes it a difficult model to characterise TASK-2.

Inglis SK *et al.* (2007) *American Journal of Physiology - Lung Cellular and Molecular Physiology*, **292**, L1304-L1312.

Authors have confirmed where relevant, that experiments on animals and man were conducted in accordance with national and/or local ethical requirements.

PC172

Age dependence of interaction between intracellular Ca^{2+}-transporting systems of permeabilized rat hepatocytes

S. Bychkova

Department of Human and Animals Physiology, Ivan Franko National University of Lviv, Lviv, Ukraine

Function of Ca2+-transporting systems could depend on animals' age. The age related features of interaction between Ca2+-transporting systems (IP3Rs, RyRs and mitochondrial Ca2+-uniporter) were investigated in rat hepatocytes. Experiments were performed using isolated hepatocytes by lidase digestion. Isolated hepatocytes were incubated with saponin for permeabilisation. Concentrations of membrane-bound Ca2+ were measured using chlortetracycline. All rats were divided on 3 different groups: young (age < 6 months, weight 0.05-0.06 kg), adult (6 months, weight 0.18-0.2 kg) and old rats (18-24 months, weight 0.45-0.50 kg).
It was shown that IP3 (10 μM) decreased the membrane-bound Ca2+ content in permeabilized hepatocytes of both young (by 27.72±9.20%; P<0.05, n=9) and old rats (by 20.47±8.23%, P<0.05, n=13), and increased the membrane-bound Ca2+ content in permeabilized hepatocytes in groups of adult rats by 15.99±5.29% (P=0.05, n=10). Ruthenium red (1μM) did not elicit significant changes in the membrane-bound Ca2+ content in hepatocytes of young and old rats, but decreased it by 22.09±7.58% (P=0.05, n=7) in groups of adult rats. Simultaneous application of IP3 and ruthenium red didn't cause statistically authentic change of membrane-bound Ca2+ content in all groups.
We also showed that ryanodine (5 nM) decreased concentration of the membrane-bound Ca2+ in permeabilized hepatocytes of young rats by 28.16±5.54% (P=0.05, n=10), old rats – by 17.95±8.66% (P<0,05, n=13), but increased the membrane-bound Ca2+ by 29.94±7.49% (P<0.05, n=8) in groups of adult rats.
In the presence of both ruthenium red and ryanodine content of membrane-bound Ca2+ in permeabilized hepatocytes was decreased by 25.52±11.03% (P<0.05, n=10) in groups of young rats. Simultaneous presence of ryanodine and ruthenium red at incubation medium caused increase of membrane-bound Ca2+ by 17.41±7.38% (P<0.05, n=13) in groups of adult rats. There was no statistically authentic change of membrane-bound Ca2+ in permeabilized hepatocytes of old rats in the presence of both ruthenium red and ryanodine.
Therefore, we observed that (1) both IP3 and ryanodine evoke age-dependent changes of membrane-bound Ca2+ content, which have similar character; (2) ruthenium red alone affected membrane-bound Ca2+ content in groups of adult rats only. The age-dependent changes of membrane-bound Ca2+ content in hepatocytes were also evoked by simultaneous application of ryanodine and ruthenium red. Thus, we conclude that there is an age-dependent interaction between Ca2+ uniporter and RyRs of hepatocytes, but the interaction between Ca2+ uniporter and IP3Rs is not age-dependent.

Authors have confirmed where relevant, that experiments on animals and man were conducted in accordance with national and/or local ethical requirements.

PC173

The effect of insulin on glucose transport in H441 human airway epithelial cells

M. Asaria, K.K. Kalsi, E.H. Baker and D.L. Baines

Basic medical Sciences, St. George's, University of London, London, UK

The effect of insulin on glucose transport in skeletal muscle, cardiac muscle and adipose tissue has long been known (1), but effects on the human bronchial epithelial cell line (H441) have not been investigated. The presence of the facilitative glucose transporter (GLUT2) in H441 cells has been identified, but the insulin-sensitive GLUT4 transporter has not been fully confirmed (2). The aim of this study was to investigate the effect of insulin on glucose uptake in H441 cells in order to help identify the presence of insulin-sensitive glucose transporters in these cells. H441 monolayers were cultured on porous filters at air interface and uptake studies were performed using 10 mM glucose with radiolabelled [^{3}H]-D-Glucose. Insulin (0-7 μM) was added either to the basolateral side or to the apical side of the monolayer 1 hour prior to glucose uptake being measured. Inhibition

of glucose transport with 1 mM phloretin (GLUT inhibitor) was also studied. Results are expressed as mean ± standard error of the mean; treatments were compared using unpaired student's t-test. Basolateral glucose uptake was 52.14 ± 19.84 nmol/mg protein with no insulin present. Maximal uptake was 484.46 ± 131.97 nmol/mg protein when 1.7 μM insulin was added to the basolateral side of the monolayer ($p<0.05$, n=5-9). The basolateral insulin concentration dose response effect was fitted with a sigmoidal curve with a Hill slope of 66.84 and a calculated EC_{50} of 1.37 μM. Glucose uptake from the apical side of the monolayer was found to be less than basolateral uptake. With no insulin, glucose uptake was 18.05 ± 5.47 nmol/mg protein and maximal uptake was 60.04 ± 10.47 nmol/mg protein when 3.4 μM insulin was added to the apical chamber ($p<0.05$, n=4-8). The apical concentration response to insulin was also sigmoidal but was different to basolateral uptake with a Hill slope of 5.4 and a calculated EC_{50} of 2.09 μM. In the presence of 1.7 μM insulin, inhibition with phloretin significantly reduced uptake from 432.68 ± 31.73 to 53.74 ± 9.55 nmol/mg protein ($p<0.001$, n=3). In conclusion, insulin stimulated basolateral and apical glucose uptake across H441 cell monolayers. These data indicate that insulin-sensitive glucose transporter(s) are present in the membranes of airway epithelial cells and inhibition with phloretin indicates that a significant component of insulin-sensitive uptake is via GLUT transporters.

Brown GK (2000). J. Inherit. Metab. Dis. 23: 237-246

Kalsi KK et al (2008) Pflugers Arch [Epub ahead of print]

This work was supported by the Wellcome Trust

Authors have confirmed where relevant, that experiments on animals and man were conducted in accordance with national and/or local ethical requirements.

WA1

Synaptic conductances and spike generation in cortical cells

H. Robinson

Department of Physiology, Development and Neuroscience, University of Cambridge, Cambridge, UK

Investigating how cortical neurons integrate their electrical inputs has commonly involved injecting fixed patterns of current and observing the resulting membrane potential and spike responses. However, we now have accurate biophysical models of the ionic conductances at the postsynaptic sites of cortical synapses and of the conductances which generate action potentials. Using conductance injection or dynamic clamp it is possible to inject point conductances which imitate the electrical properties of synaptic inputs, including the shunting, reversible nature of inhibitory GABAA receptor input, the saturating or "choking" behaviour of AMPA receptor input; and the voltage-dependent block of NMDA receptor input. Complex conductance signals which reproduce the effects of stochastic and oscillatory network firing can be applied repeatedly and with high precision. In this talk, I review our work using this approach, addressing the nature of the threshold and of reliability of spike generation in cortical neurons, how synaptic conductance input patterns are encoded into variations in action potential shape, and how neurons integrate network burst and gamma oscillatory activity.

Robinson, HPC and Kawai N (1993) Injection of digitally synthesized synaptic conductance transients to measure the integrative properties of neurons. J. Neuroscience Meth. 49:157-165.

Harsch A and Robinson HPC (2000) Postsynaptic variability of firing in rat cortical neurons: the roles of input synchronization and synaptic NMDA receptor conductance. J. Neurosci. 20:6181-6192.

Polavieja GG de, Harsch A, Kleppe I, Robinson HPC and Juusola M (2005) Stimulus history reliably shapes action potential waveforms of cortical neurons. J. Neurosci. 25:5657-5665.

Tateno T and Robinson HPC (2006) Rate coding and spike-time variability in cortical neurons with two types of threshold dynamics. J Neurophysiol 95: 2650–2663.

Robinson HPC (2007) A scriptable DSP-based system for dynamic conductance injection. J. Neurosci. Meth. 169:271-281.

Morita K, Kalra R, Aihara K and Robinson HPC (2008) Recurrent synaptic input and the timing of gamma-frequency-modulated firing of pyramidal cells during neocortical "UP" states. J. Neurosci. 28:1871-1881.

Authors have confirmed where relevant, that experiments on animals and man were conducted in accordance with national and/or local ethical requirements.

WA2

The dendritic dynamic clamp – a tool to investigate dendritic synaptic integration

S. Williams

MRC LMB, Cambridge, UK

The dynamic clamp can be used to mimic the operation of synapses. Recently we have used this technique to emulate synaptic activity at somatic and / or apical dendritic sites of neocortical pyramidal neurons. Using dual dendritic recording techniques, synaptic activity can be accurately generated at apical dendritic sites using closely spaced (<10 μm) electrodes for current injection and voltage recording. We have confirmed the operation of this system using somatic voltage clamp recordings, a procedure that has also allowed us to address the limitations of somatic voltage clamp recording in central neurons. Using the dendritic dynamic clamp approach we have investigated the somatic impact of inhibitory and excitatory synaptic activity generated from determined dendritic sites (up to 750 μm form the soma). Furthermore we have been able to show how conductance and voltage are differentially compartmentalised in the dendritic tree. Results indicate that neocortical pyramidal neurons operate with (at least) two independent compartments for synaptic integration - a somatic compartment and an apical dendritic compartment. Communication from the apical dendritic compartment to the soma and axon is not mediated by the direct spread of synaptic activity, but rather by the forward propagation of dendritic spikes.

Medical Research Council